

FILE COPY

(4)

REPORT SD-TR-89-09

AD-A206 227

# X-Ray Spectrophotometric Remote Sensing of Diffuse Auroral Ionization

R. R. VONDRAK and R. M. ROBINSON  
Lockheed Palo Alto Research Laboratory  
3251 Hanover Street  
Palo Alto, CA 94304

and

P. F. MIZERA and D. J. GORNEY  
Space Sciences Laboratory  
Laboratory Operations  
The Aerospace Corporation  
El Segundo, CA 90245

20 March 1989

Prepared for

SPACE DIVISION  
AIR FORCE SYSTEMS COMMAND  
Los Angeles Air Force Base  
P.O. Box 92960  
Los Angeles, CA 90009-2960

DTIC  
SELECTED  
S E D  
CE

APPROVED FOR PUBLIC RELEASE;  
DISTRIBUTION UNLIMITED

89 4 03 035

UNCLASSIFIED

SECURITY CLASSIFICATION OF THIS PAGE

REPORT DOCUMENTATION PAGE

1a. REPORT SECURITY CLASSIFICATION Unclassified			1b. RESTRICTIVE MARKINGS			
2a. SECURITY CLASSIFICATION AUTHORITY			3. DISTRIBUTION / AVAILABILITY OF REPORT Approved for public release; distribution unlimited.			
2b. DECLASSIFICATION / DOWNGRADING SCHEDULE						
4. PERFORMING ORGANIZATION REPORT NUMBER(S) TR-0088(3940-06)-3			5. MONITORING ORGANIZATION REPORT NUMBER(S) SD-TR-89-09			
6a. NAME OF PERFORMING ORGANIZATION The Aerospace Corporation Laboratory Operations		6b. OFFICE SYMBOL (if applicable)	7a. NAME OF MONITORING ORGANIZATION Space Division			
6c. ADDRESS (City, State, and ZIP Code) El Segundo, CA 90245			7b. ADDRESS (City, State, and ZIP Code) Los Angeles Air Force Base Los Angeles, CA 90009-2960			
8a. NAME OF FUNDING / SPONSORING ORGANIZATION		8b. OFFICE SYMBOL (if applicable)	9. PROCUREMENT INSTRUMENT IDENTIFICATION NUMBER F04701-85-C-0086-P00019			
8c. ADDRESS (City, State, and ZIP Code)			10. SOURCE OF FUNDING NUMBERS			
			PROGRAM ELEMENT NO.	PROJECT NO.	TASK NO.	WORK UNIT ACCESSION NO.
11. TITLE (Include Security Classification) X-Ray Spectrophotometric Remote Sensing of Diffuse Auroral Ionization						
12. PERSONAL AUTHOR(S) Vondrak, R. R., Robinson, R. M., Mizera, P. F., Gorney, D. J.						
13a. TYPE OF REPORT		13b. TIME COVERED FROM _____ TO _____		14. DATE OF REPORT (Year, Month, Day) 1989 March 20	15. PAGE COUNT 22	
16. SUPPLEMENTARY NOTATION						
17. COSATI CODES			18. SUBJECT TERMS (Continue on reverse if necessary and identify by block number) Aurora ; Ionosphere ; Bremsstrahlung x rays ; Remote sensing			
FIELD	GROUP	SUB-GROUP				
19. ABSTRACT (Continue on reverse if necessary and identify by block number) Auroral electron precipitation produces both E-region ionization and bremsstrahlung x rays. In a set of coordinated observations these atmospheric effects of electron precipitation were measured simultaneously by the x-ray sensor on the DMSP/F2 spacecraft and by the incoherent-scatter radar at Chatanika, Alaska. In all data sets there was good agreement between the locations of the x-ray source regions and the regions of enhanced E-region ionization. Detailed comparisons were made between the measured and derived altitude profiles of ionization for two auroral conditions, a premidnight auroral band and a sunlit diffuse aurora. These comparisons validate the ability to derive auroral ionization from satellite-based x-ray measurements. <i>Keywords:</i>						
20. DISTRIBUTION / AVAILABILITY OF ABSTRACT <input checked="" type="checkbox"/> UNCLASSIFIED/UNLIMITED <input type="checkbox"/> SAME AS RPT <input type="checkbox"/> DTIC USERS			21. ABSTRACT SECURITY CLASSIFICATION Unclassified			
22a. NAME OF RESPONSIBLE INDIVIDUAL			22b. TELEPHONE (Include Area Code)		22c. OFFICE SYMBOL	

PREFACE

The Chatanika radar is operated by SRI International for the National Science Foundation. This work is supported at Lockheed under support from the Office of Naval Research, the Johns Hopkins University Applied Physics Laboratory (Contract APL 602225-L), and the Lockheed Independent Research Program.

Accession For	
NTIS GRA&I	<input checked="" type="checkbox"/>
DTIC TAB	<input type="checkbox"/>
Unannounced	<input type="checkbox"/>
Justification	
By	
Distribution/	
Availability Codes	
Dist	Avail and/or Special
A-1	

CONTENTS

PREFACE . . . . . 1

INTRODUCTION . . . . . 5

DETERMINATION OF AURORAL ELECTRON FLUXES FROM X RAYS . . . . . 6

DESCRIPTION OF EXPERIMENTS . . . . . 8

OBSERVATIONS OF AN EVENING AURORA . . . . . 9

OBSERVATIONS OF A SUNLIT MORNING AURORA . . . . . 14

SUMMARY AND DISCUSSION . . . . . 20

REFERENCES . . . . . 22

FIGURES

1.	DMSF groundtrack over Alaska on 21 February 1979 . . . . .	10
2.	Contour plot of electron densities as a function of altitude and invariant latitude measured by the radar during a meridian scan on 21 February 1979 . . . . .	11
3.	X-ray fluxes and measured and derived electron fluxes and electron density for the evening sector auroral band . . . . .	13
4.	DMSF groundtrack over Alaska on 15 June 1978 . . . . .	15
5.	Contour plot of electron densities as a function of altitude and invariant latitude measured by the radar during the meridian scan on 15 June that was simultaneous with the DMSF satellite crossing . . . . .	16
6.	Variation of peak E-region density with latitude and magnetic local time as inferred from nine consecutive radar elevation scans . . . . .	17
7.	X-ray fluxes measured by DMSF, height profile of ionization production rate due to kilovolt electrons and sunlight, and measured and derived electron densities for the morning sector sunlit diffuse aurora . . . . .	18

## INTRODUCTION

Ionization in the earth's atmosphere is produced primarily by solar illumination and incoming energetic particles. Ionization produced by solar illumination is well understood and can be accurately modeled. But at high latitudes, particularly at night, the dominant source of ionization may be precipitating protons and electrons with energies less than about 100 keV. This makes modeling high latitude ionization difficult because these particle fluxes may be temporally and spatially varying. Global specification of the distribution of ionization at high latitudes is best done using detectors on space-based platforms capable of viewing a large portion of the earth at one time. This method involves detecting electromagnetic radiation originating from the impact of charged particles into the atmosphere. This radiation may be in the X-ray, ultraviolet, or visible portion of the spectrum. The X-ray and ultraviolet techniques hold great promise for remotely sensing ionization because of the absence of a background emission source that prohibits imaging of aurorally produced emissions in the sunlit hemisphere. However, detailed comparisons between modeled and measured auroral emissions are required to assess the accuracy of these techniques.

In this paper we compare simultaneous measurements by the Chatanika radar and the DMSP-F2 satellite X-ray detector to demonstrate that remote X-ray observations can be used to determine the ionization produced by auroral electron precipitation. The accuracy of the X-ray remote sensing is assessed by a quantitative comparison between the profiles of ionization measured by the ground-based incoherent-scatter radar and the profiles derived from the satellite-based X-ray measurements. Measurements were made under a variety of auroral conditions, including dynamic evening aurora and sunlit diffuse aurora in the morning.

The next section of this paper describes the method by which auroral electron fluxes are calculated from X-ray measurements. The following sections describe radar and satellite data obtained during two auroral events: an evening pass on 21 February 1979 and a morning pass on 15 June 1978. The concluding section summarizes the results and discusses the utility of the X-ray remote sensing method.

## DETERMINATION OF AURORAL ELECTRON FLUXES FROM X-RAYS

Precipitating electrons interact with the atmosphere to produce ionization and various forms of electromagnetic radiation. Excitation of neutral and ionic constituents caused by impact of primary and secondary electrons leads to optical emissions at virtually all wavelengths. In addition, the slowing down of the primary electrons produces bremsstrahlung X-ray emission. The calculation of ionization produced by the precipitating electrons is done by determining their spectral distribution from the measured emissions. Because we are here restricting our discussion to altitudes between 80 and 200 km, the electron energy range of interest is approximately 500 eV to 100 keV. Once the electron spectral distribution is known, the resulting ionization can be accurately modeled (see, for example, Vondrak and Robinson, 1985). Thus, remote sensing depends on the accuracy with which the energy distribution of the precipitating electrons can be determined from the measured emissions.

The flux of X-rays  $F_x$  of energy  $E_x$  is given by

$$F_x(E_x) = \int_{E_x}^{\infty} \Phi(E_x, E_e) F_e(E_e) dE_e \quad (1)$$

where  $F_e$  is the flux of electrons of energy  $E_e$ . The function  $\Phi(E_x, E_e)$  is a source function relating the two fluxes. In this expression, absorption of X-rays in the atmosphere is neglected; this is justified for most auroral electron spectra where the average energy of the electrons is well below about 40 keV. Determination of the electron fluxes from the measured X-ray fluxes involves deconvolution of this integral equation. There have been several approaches to this problem. For the experiments described below we use the inversion technique described by Brown (1972). In this method, the differential cross-section for X-ray bremsstrahlung production is given by the Bethe-Heitler formula. The expression for calculating the flux of X-rays produced by a given distribution of electrons is in a form that can be inverted analytically. Thus, if the X-ray fluxes are known, the electron spectrum can be derived from the measured X-ray spectrum by a direct calculation. Because the method involves taking derivatives and second derivatives of the X-ray distribution, it is sensitive to uncertainties in the measured X-ray intensities. In the data used here, the measured X-ray fluxes were integrated over times long enough to ensure good counting statistics. All methods for deconvolving X-ray spectra result in electron spectra with large

uncertainties at the lower energies. This is because the low energy X-rays are produced primarily by higher energy electrons. Fortunately, the resulting electron density profiles in the ionosphere below 200 km altitude are relatively insensitive to the low energy electron fluxes, so that the densities can be determined with good precision.

## DESCRIPTION OF EXPERIMENTS

The ground-based ionization measurements were made with the Chatanika incoherent-scatter radar (Leadabrand et al., 1972; Baron, 1977; Vondrak, 1983). For these experiments the radar was generally operated in a variety of modes combining elevation scans and fixed-position measurements. The ionization was measured with a range resolution of 4.5 km and with integration times of about 15 sec. Because the satellite and radar measurements are generally not spatially coincident nor simultaneous, ground-based all-sky photographs were used when possible to relate the measurements made during the nighttime passes. Visible auroral imagery from the DMSP-F2 satellite was not available for the cases used in this study.

X-ray measurements were made with an auroral X-ray sensor on the DMSP-F2 satellite (Mizera et al., 1978). DMSP-F2 is in a nearly sun-synchronous circular polar orbit at an altitude of 830 km. The sensor field of view is  $2^\circ$  by  $14^\circ$ , providing an in-track spatial resolution of about 50 km and a cross-track resolution of about 350 km. This corresponds to about  $0.5^\circ$  of latitude by about 0.5 hour of local time. The downlooking X-ray sensor provides integral X-ray measurements in fifteen energy channels from 1.4 to 20 keV. These X-ray spectra were converted to equivalent incident electron spectra using the inversion technique described by Brown (1972). From these electron spectra we calculated the ionization production rate  $q$  as a function of altitude using the method of Rees (1963). The electron density  $n$  was calculated assuming the model effective recombination coefficient  $\alpha$  given by Vickrey et al. (1982). A transport-free equilibrium solution was used for the electron continuity equation, such that the electron density as a function of altitude  $z$  is given by

$$n(z) = \left[ \frac{q(z)}{\alpha(z)} \right]^{\frac{1}{2}} \quad (2)$$

For the sunlit cases the production rate due to electron precipitation was added to the solar photoionization rate specified in the empirical model of Robinson and Vondrak (1984).

Precipitating electron fluxes in eight differential energy channels from 1-20 keV were measured once per second by the J/3 instrument on DMSP. Whenever available, the precipitating electron data were used as an independent test of the validity of the X-ray spectral inversion technique (see also, Mizera and Gorney, 1982).

The entire set of simultaneous Chatanika/DMSP-F2 observations was searched for cases that satisfy the criteria of spatial and temporal coincidence, with aurora present

within the Chatanika field of view. Another constraint was that the auroral luminosity and ionization had to be fairly homogenous over the X-ray sensor field of view. Only four cases were identified that met these criteria. In all cases there was good spatial coincidence between the regions of enhanced X-ray luminosity and the regions of enhanced ionization. During two cases the conditions of simultaneity and homogeneity were sufficiently good to allow a detailed quantitative comparison between the measured and inferred altitude profiles of ionization. In the next section we present in detail the observations made on these two days that are representative of auroral conditions in the evening sector and in the morning sunlit sector.

## OBSERVATIONS OF AN EVENING AURORA

On 21 February 1979 the DMSP-F2 satellite passed slightly to the east of Chatanika at 0727 UT (2127 local time). The location of the satellite ground track is shown in Figure 1. During that night the Chatanika radar was operated in alternating elevation scans and fixed-position measurements. The E-region limits of the elevation scan closest in time to the satellite pass are also shown in Figure 1.

During the DMSP pass there were bright auroral bands south and overhead of Chatanika. Following the satellite pass, the bright auroral bands moved southward. The Chatanika elevation scan began in the south within one of the bright auroral bands. All-sky camera photographs taken at that time showed that the auroral bands extended over the southern sky from the northwest to the southeast as shown by the shaded region in Figure 1. On the figure are shown the times corresponding to the beginning and end of the radar elevation scan. As the radar scanned northward the auroral conditions changed dramatically with the sudden appearance of rayed arcs and reduced auroral luminosity. These temporal variations were evident both in the all-sky photographs and in the Chatanika measurements made in the fixed-position mode and during the elevation scan.

The radar ionization measurements during the elevation scan closest in time to the satellite pass are shown in Figure 2. The contours show electron density as a function of altitude and invariant latitude in the magnetic meridian plane. Conspicuous features are the enhanced ionization between  $62^\circ$  and  $66^\circ$  latitude that is associated with the bright visible auroral band and the high-altitude ionization in the north between  $66.6^\circ$  and  $67.2^\circ$ . This latter ionization is associated with the rayed arcs that appeared after the satellite pass. The peak E-region electron density in the bright auroral band varied between  $3 \times 10^5 \text{ cm}^{-3}$

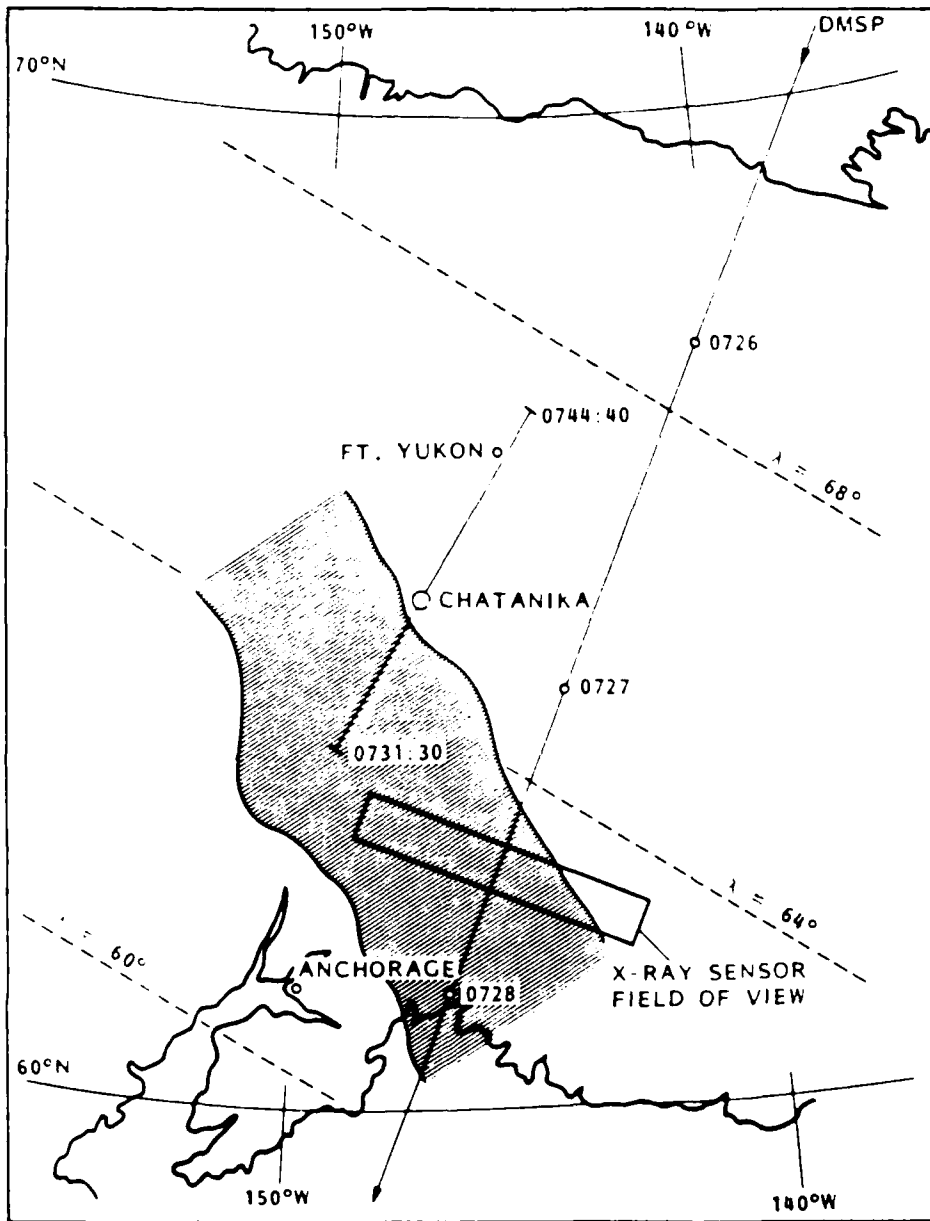


Figure 1. DMSp groundtrack over Alaska on 21 February 1979. The location of the bright auroral band at 0732 UT is shaded. Also shown are the E-region limits of the Chatanika radar elevation scan and the field of view of the DMSp X-ray sensor.

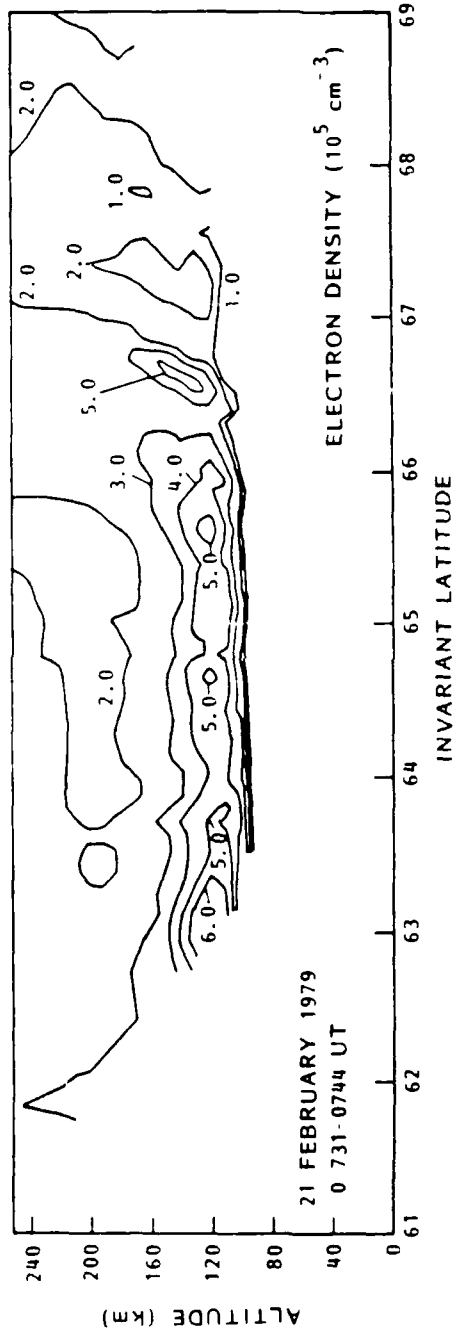


Figure 2. Contour plot of electron densities as a function of altitude and invariant latitude measured by the radar during a meridian scan on 21 February 1979. The scan began a few minutes after the passage of the DMSP satellite.

and  $6 \times 10^5 \text{ cm}^{-3}$  and was situated at altitudes between 110 and 120 km. Electron densities in the rayed arcs maximized at altitudes near 140 km.

The X-ray sensor on the DMSP satellite detected enhanced X-ray fluxes at the latitudes near Chatanika. Because of the temporal variations in the aurora after the satellite pass, we compare the radar and satellite measurements made in the bright auroral band to the south of Chatanika which remained relatively stable. The energy distribution of bremsstrahlung X-rays in the auroral band south of Chatanika is shown in the first panel of Figure 3. The measurements are shown by the individual points with error bars derived from counting statistics. The instantaneous field of view of the detector is shown by the rectangle in Figure 1. The X-ray data were integrated for only three seconds so that the total field of view was about 40 per cent larger in the direction of satellite motion than indicated on the figure. Because of the large field of view of the X-ray sensor, the measured X-ray energy distribution represents a spatial average of the X-ray fluxes produced in the band.

The precipitating electron energy distribution derived from the X-ray distribution in the auroral band is shown in the middle panel of Figure 3. For comparison we show in Figure 3 the direct measurement of the precipitating electron flux by the J/3 electron detector on DMSP. The J/3 electron measurements were made on the same field lines as the X-ray sensor field of view and were averaged over a time interval that corresponds to the X-ray sensor field of view along the satellite ground track divided by the satellite velocity. Good agreement is evident; both the measured and derived spectra indicate average electron energies of about 7 keV with a total energy flux of  $10.8 \text{ ergs/cm}^2\text{-s}$ .

The third panel in Figure 3 shows the ionization profile computed from the electron fluxes that were determined from the X-ray data. For comparison we show the average electron density measured by the radar over the latitude range that overlaps with the X-ray sensor field of view. The horizontal bars show one standard deviation from the mean value. It is apparent that the electron density was fairly uniform within the X-ray sensor field of view. The agreement between the measured electron densities and the derived electron densities is very good at all altitudes. We expect the densities computed from the X-rays to be slightly less than the measured densities because the auroral bands did not quite fill the detector field of view, as shown in Figure 1.

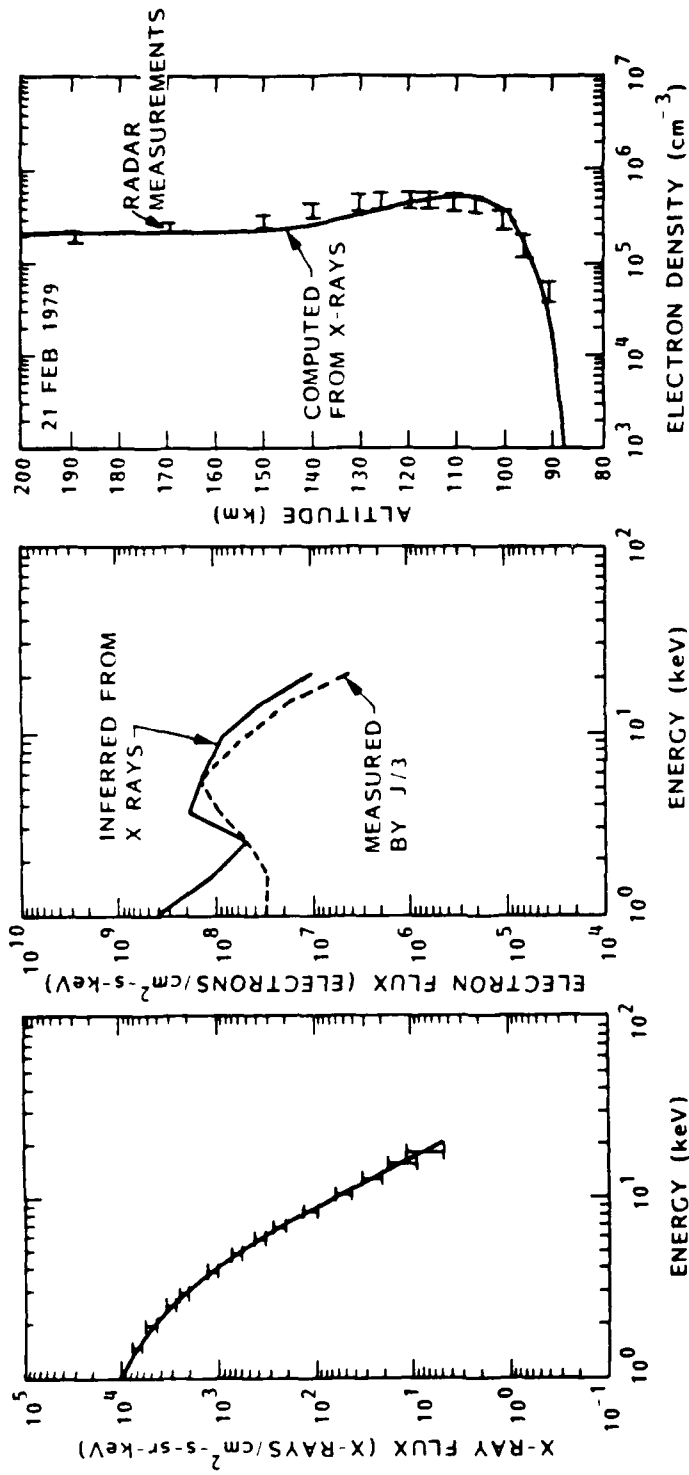


Figure 3. X-ray fluxes and measured and derived electron fluxes and electron density for the evening sector auroral band. Error bars are shown on the DMSP X-ray and electron flux measurements. The horizontal bars on the radar measurements indicate the results of spatially averaging the data over latitudes appropriate to the X-ray detector field of view.

## OBSERVATIONS OF A SUNLIT MORNING AURORA

On 15 June 1978 the DMSP satellite passed to the east of Chatanika, intersecting the Chatanika magnetic meridian at 1547 UT (0547 local time on 16 June). The DMSP ground track is shown in Figure 4. Because the day of this experiment is close to the summer solstice, sunrise at Chatanika was more than four hours prior to the DMSP pass. The solar zenith angle at Chatanika was about  $70^\circ$  during the satellite pass.

The Chatanika radar was operated in continuous sequential elevation scans for several hours before and after the satellite crossing. Figure 5 shows the latitudinal distribution of ionization measured during the elevation scan made at the time of the pass. A broad region of diffuse aurora is visible over Chatanika with maximum ionization of about  $3 \times 10^5 \text{ cm}^{-3}$  between 115 and 120 km altitude. Thus, the average energy of the electrons producing the ionization was similar to that observed during the evening aurora described above. Because no visible auroral imagery was available for this sunlit case, we examined data from successive elevation scans to determine the stability of the auroral precipitation during the satellite pass. In Figure 6 we show the maximum E region electron density measured by the radar during nine consecutive elevation scans. The data are plotted as a function of invariant latitude and magnetic local time. The DMSP trajectory is shown by the solid line slanting toward the upper left part of the figure. The location of the Chatanika measurements made during the meridian scan that was simultaneous with the satellite ground track is shown by the solid line in the left part of the figure. Along the satellite ground track we show a rectangle indicating the X-ray sensor field of view for the integration period during which the maximum X-ray flux was measured. The dashed portion of the rectangle represents the increase in the size of the field of view owing to the satellite motion during the six seconds over which the X-ray data were integrated. Note that the field of view does not overlap the Chatanika radar field of view during the scan that was simultaneous with the satellite pass. However, the data from successive scans shows that there was only a small change in maximum E region density at later local times.

The X-ray spectral distribution measured by the DMSP instrument during the satellites passage over the diffuse aurora is shown in the first panel of Figure 7. As in Figure 3, the vertical bars show the uncertainty in the measurements and the solid line is a fit to the data. Comparing this spectral distribution with that shown in Figure 3 shows that the spectral shapes are very similar, with the morning sector fluxes lower by about a factor of

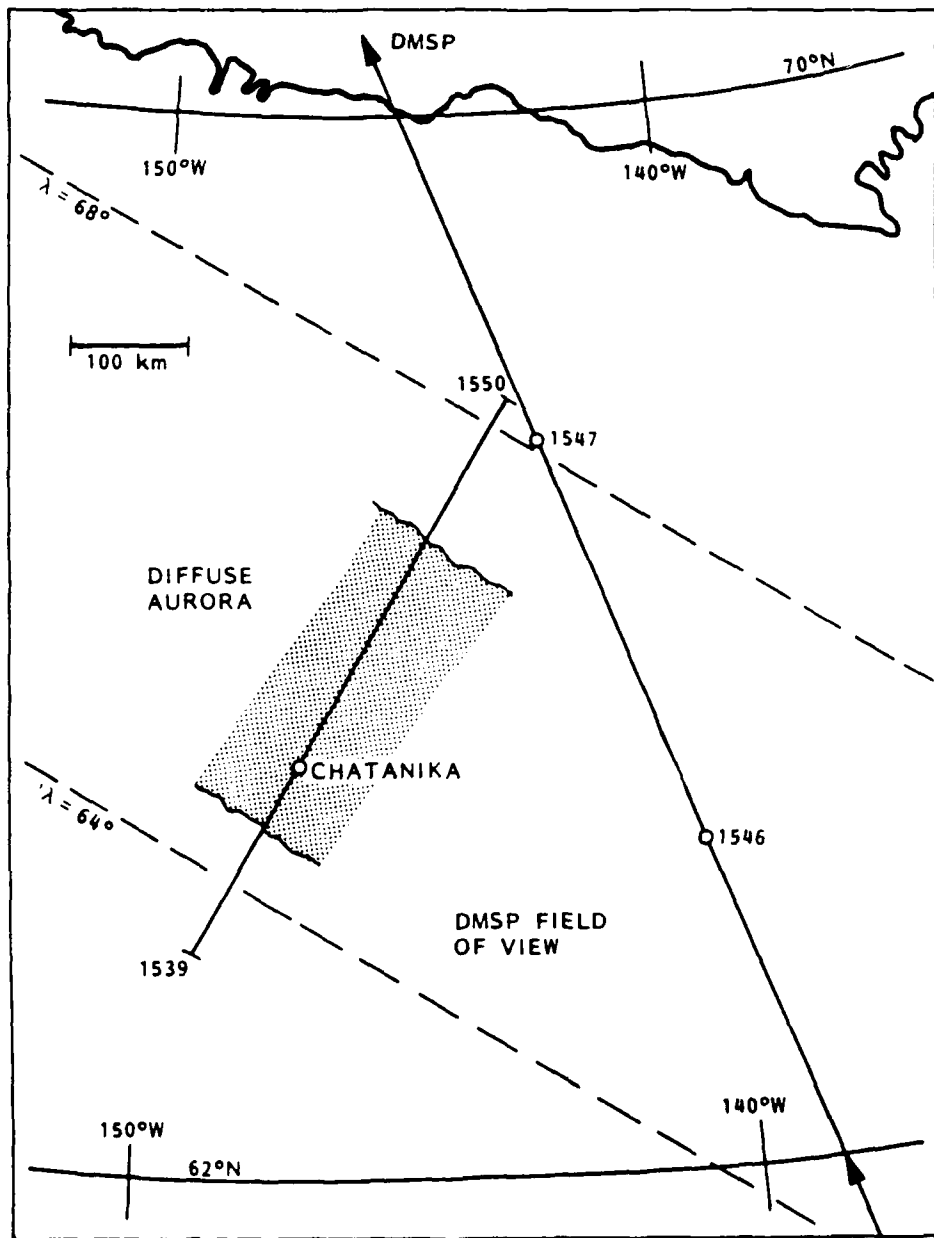


Figure 4. DMSP groundtrack over Alaska on 15 June 1978. The Chatanika field of view during a meridian scan that was simultaneous with the satellite pass is also shown. The shaded region indicates the latitudinal extent of the diffuse aurora.

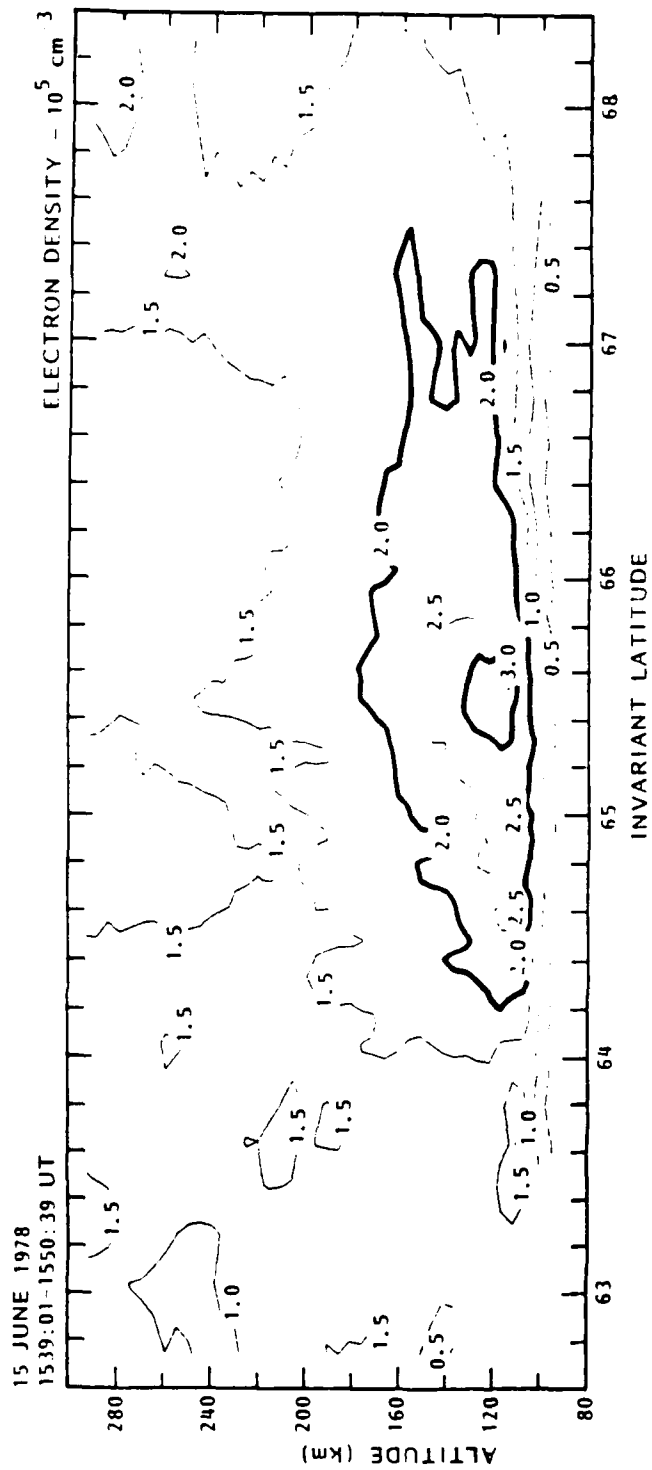


Figure 5. Contour plot of electron densities as a function of altitude and invariant latitude measured by the radar during the meridian scan on 15 June that was simultaneous with the DMSP satellite crossing.

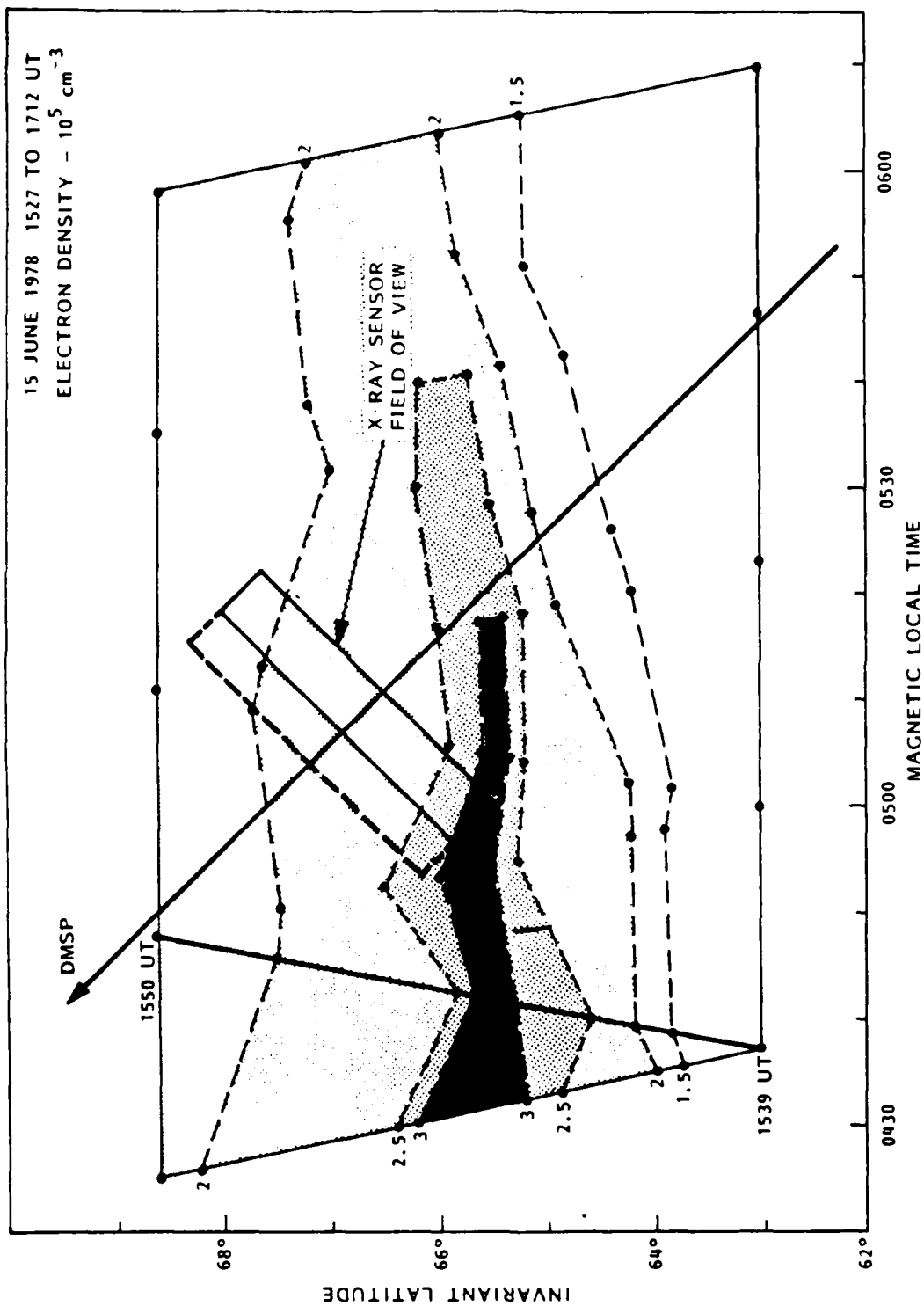


Figure 6. Variation of peak E-region density with latitude and magnetic local time as inferred from nine consecutive radar elevation scans. The DMSP satellite groundtrack in this coordinate system is also shown along with the field of view of the X-ray detector during the integration period that yielded the maximum X-ray flux.

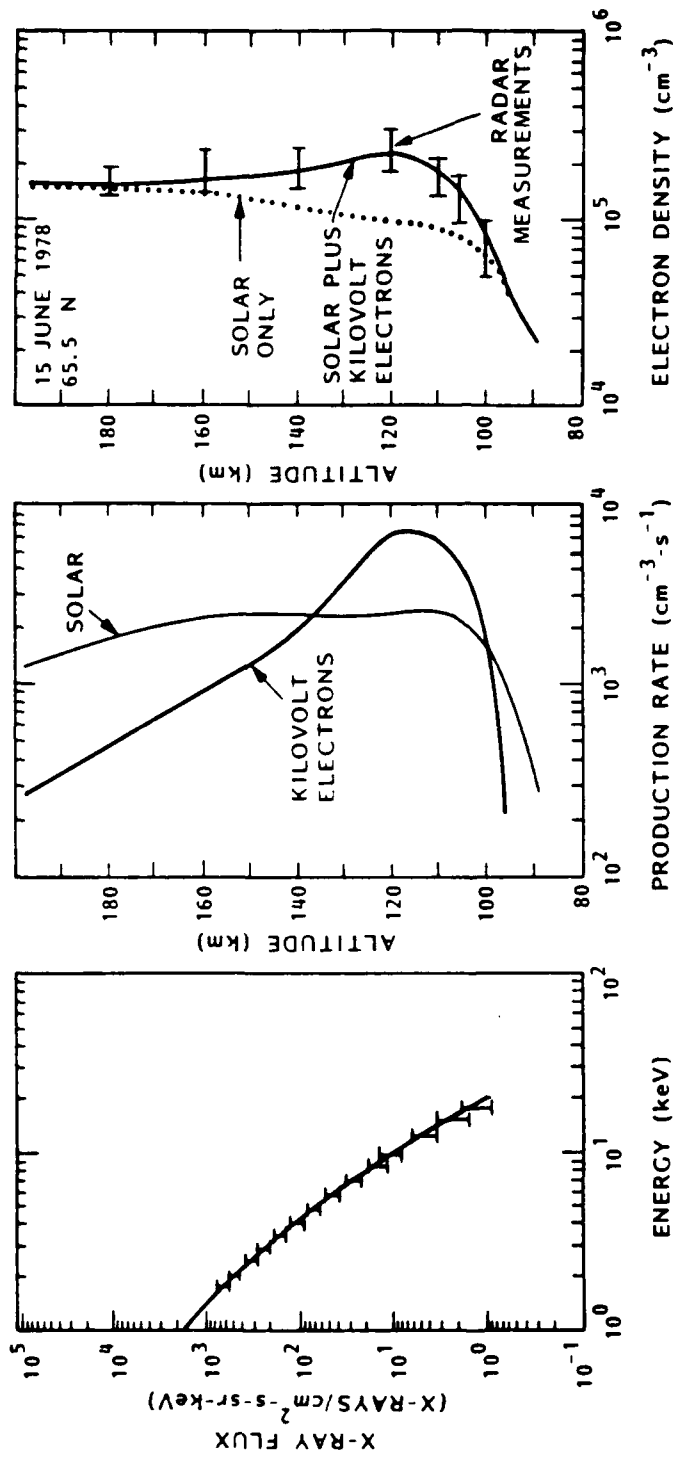


Figure 7. X-ray fluxes measured by DMSP, height profile of ionization production rate due to kilovolt electrons and sunlight, and measured and derived electron densities for the morning sector sunlit diffuse aurora. Error bars are shown on the X-ray measurements. The horizontal bars on the radar measurements indicate the range in electron densities measured across the diffuse aurora.

seven from those measured in the evening sector event. The calculated electron spectrum has an average energy of about 6 keV and energy flux of  $1.5 \text{ ergs/cm}^2\text{-s}$ . The middle panel of Figure 7 shows the production rate of ionization resulting from the derived electron fluxes. The peak ionization rate occurs near 115 km altitude and falls off rapidly at altitudes above the peak. However, solar illumination must also be taken into account in estimating the observed ionization. The rate of ionization produced by solar illumination for a solar zenith angle of  $70^\circ$  was determined using the results of Robinson and Vondrak (1984) and is shown in the middle panel of Figure 7. Although the ionization produced near the E region peak by sunlight is small compared to that produced by precipitating electrons, the solar contribution is dominant at higher altitudes. The resulting electron densities are shown in the third panel of Figure 7. Because the X-ray detector field of view encompassed almost the entire diffuse aurora at the time of the measurement, we show for comparison the range in electron densities measured by the radar across the diffuse auroral region. The derived profile falls well within the range observed by the radar. We note, in particular, the importance of adding in the contribution from solar illumination in obtaining the agreement at the higher altitudes.

## SUMMARY AND DISCUSSION

The comparative analysis of the Chatanika/DMSP data sets shows that satellite-borne X-ray measurements can be used to determine quantitatively the spatial distribution of electron energy deposition and ionization in the auroral ionosphere. For all the cases that were analyzed, the X-ray measurements could be used to identify the regions of electron energy deposition measured independently with the Chatanika radar and the all-sky camera. For two of the cases, auroral conditions were sufficiently uniform and stable to allow a detailed comparison between electron densities determined from derived energetic electron fluxes and electron densities measured directly by incoherent scatter radar. The data were obtained during observations of an active evening sector aurora and a morning sector diffuse aurora. The average energy of the precipitating electrons in both cases was about 6 keV in the most intense regions. The energy flux in the morning sector event was lower by about a factor of seven from that in the evening sector event. This difference in the calculated energy flux was consistent with the factor of two to three difference in the observed E-region peak electron density. Because the morning sector aurora was sunlit, the contribution to the total ionization produced by photoionization had to be added to bring the derived and measured profiles into agreement. This is the first time quantitative remote sensing of ionization in a sunlit aurora has been accomplished.

In the two cases described in detail above, the X-ray measurements represented spatial averages because of the large field of view of the detector. Thus, the computed profiles were compared with electron densities measured by the radar during a scan over a latitudinal range consistent with the X-ray detector field of view. The agreement between the derived and measured densities depends on a combination of statistical accuracy of the measurements, temporal variations of the ionosphere, inhomogeneities over the satellite sensor field of view, and uncertainties in the calculation of ionization from the bremsstrahlung measurements. An additional uncertainty in the X-ray remote sensing technique is the presence of proton precipitation. Although electrons are the dominant source of ionization in the aurora on a global basis, precipitating protons can occasionally produce comparable or even greater amounts of ionization (Basu et al., 1987). Because precipitating protons produce no bremsstrahlung X-rays, their presence and the associated ionization cannot be detected by the DMSP X-ray imager.

Despite these uncertainties, it is obvious from our results that the X-ray remote sens-

ing technique holds great promise for monitoring auroral electron precipitation on a global basis. Because the X-ray technique also yields information about the spectral distribution of the auroral electrons, these measurements can be used to determine the height profile of electron density at altitudes below 200 km. Further observations of the type described above are important in establishing the range in auroral conditions under which the technique is applicable.

## REFERENCES

- Baron, M. J., The Chatanika Radar System, in *Radar Probing of the Auroral Plasma*, [Proceedings of the EISCAT Summer School, Tromso, Norway, June 5-13, 1975], A. Brekke, ed., pp. 385-405 (Universitetsforlaget, Tromso-Oslo-Bergen, 1977).
- Basu, B., J. Jasperse, R. Robinson, R. Vondrak and D. Evans, Linear transport theory of auroral proton precipitation: A comparison with observations, *J. Geophys. Res.*, **92**, 5920, 1987.
- Brown, J. C., The deduction of energy spectra of non-thermal electrons in flares from the observed dynamic spectra of hard X-ray bursts, *Solar Phys.*, **18**, 489, 1972.
- Leadabrand, R. L., M. J. Baron, J. Petriceks and H. F. Bates, Chatanika, Alaska, auroral zone incoherent scatter facility, *Radio Science*, **7**, 747, 1972.
- Mizera, P. F., J. G. Luhmann, W. A. Kolasinski, and J. B. Blake, Correlate observations of auroral arcs, electrons, and X-rays from a DMSP satellite, *J. Geophys. Res.*, **83**, 5573, 1978.
- Mizera, P. F. and D. J. Gorney, X-rays from the aurora, Proc. European Geophysical Society, Polar Aurora Symposium, Leeds, England, 1982.
- Rees, M. H., Auroral ionization and excitation by incident energetic electrons, *Planet. Space Sci.*, **11**, 1209, 1963.
- Robinson, R. M., and R. R. Vondrak, Measurements of E-region ionization and conductivity produced by solar illumination at high latitudes, *J. Geophys. Res.*, **89**, 3951, 1984.
- Vickrey, J. F., R. R. Vondrak and S. J. Matthews, Energy deposition by precipitating particles and Joule dissipation in the auroral ionosphere, *J. Geophys. Res.*, **87**, 5184, 1982.
- Vondrak, R. R., Incoherent-scatter radar measurements of electric field and plasma in the auroral ionosphere, in *High Latitude Space Plasma Physics*, B. Hultqvist and T. Hagfors, ed., Plenum Press, N.Y., p. 73-94, (1983).
- Vondrak, R. R. and R. M. Robinson, Inference of high latitude ionization and conductivity from AE-C measurements of auroral electron fluxes, *J. Geophys. Res.*, **90**, 7505, 1985.